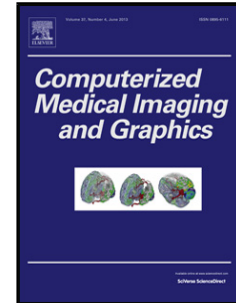


Accepted Manuscript

Title: Computer Aided Diagnosis of Degenerative Intervertebral DiscDiseases from Lumbar MR Images

Author: Ayse Betul Oktay Nur Banu Albayrak Yusuf Sinan Akgul



PII: S0895-6111(14)00057-3
DOI: <http://dx.doi.org/doi:10.1016/j.compmedimag.2014.04.006>
Reference: CMIG 1257

To appear in: *Computerized Medical Imaging and Graphics*

Received date: 30-11-2013
Revised date: 2-4-2014
Accepted date: 30-4-2014

Please cite this article as: Ayse Betul Oktay, Nur Banu Albayrak, Yusuf Sinan Akgul, Computer Aided Diagnosis of Degenerative Intervertebral DiscDiseases from Lumbar MR Images, *Computerized Medical Imaging and Graphics* (2014), <http://dx.doi.org/10.1016/j.compmedimag.2014.04.006>

This is a PDF file of an unedited manuscript that has been accepted for publication. As a service to our customers we are providing this early version of the manuscript. The manuscript will undergo copyediting, typesetting, and review of the resulting proof before it is published in its final form. Please note that during the production process errors may be discovered which could affect the content, and all legal disclaimers that apply to the journal pertain.

Computer Aided Diagnosis of Degenerative Intervertebral Disc Diseases from Lumbar MR Images

Ayse Betul Oktay^{a,*}, Nur Banu Albayrak^b, Yusuf Sinan Akgul^b

^a*Department of Computer Engineering,
Istanbul Medeniyet University
Istanbul, Turkey*

^b*GIT Vision Lab, <http://vision.gyte.edu.tr/>
Department of Computer Engineering,
Gebze Institute of Technology, Gebze, Kocaeli, Turkey*

Abstract

This paper presents a novel method for the automated diagnosis of the degenerative intervertebral disc disease in midsagittal MR images. The approach is based on combining distinct disc features under a machine learning framework. The discs in the lumbar MR images are first localized and segmented. Then, intensity, shape, context, and texture features of the discs are extracted with various techniques. A Support Vector Machine classifier is applied to classify the discs as normal or degenerated. The method is tested and validated on a clinical lumbar spine dataset containing 102 subjects and the results are comparable to the state of the art.

Keywords: Degenerative disc disease, machine learning, intervertebral disc, herniation, desiccation, degeneration, computer aided diagnosis

1. Introduction

The intervertebral discs are structures between the adjacent vertebrae which absorb stress and shock during the body movements and prevent the vertebrae from grinding against one another. An intervertebral disc is com-

*Corresponding Author

Email addresses: abetul.oktay@medeniyet.edu.tr (Ayse Betul Oktay),
albayrak@bilmuh.gyte.edu.tr (Nur Banu Albayrak), akgul@bilmuh.gyte.edu.tr
(Yusuf Sinan Akgul)

Preprint submitted to Computerized Medical Imaging and Graphics

April 2, 2014

1
2
3
4
5
6
7
8
9 posed of two parts: the nucleus pulposus and the annulus fibrosis. The
10 nucleus pulposus is the jelly-like elastic center of the disc and it has a high
11 water content. The annulus fibrosis, consisting of collagen fibers, is the outer
12 shell and it encloses the nucleus pulposus.
13

14 There may be pathologies at the intervertebral discs. For example, the
15 annulus fibrosis may be injured because of several factors like aging, trauma,
16 mechanical loading, etc., and tears may occur. Nucleus pulposus may lose
17 its elastic content by leaking through the tear and it may dry up. Then,
18 it collapses and cannot act as a shock absorber. This causes low back pain
19 which is one of the most common health problems. In the United States,
20 nearly 50 billion dollars is spent annually for the evaluation and treatment
21 of low back pain [1, 2]. A Computer Aided Diagnosis (CAD) system for
22 intervertebral disc diseases would provide quick screening and might also
23 detect the abnormalities that a radiologist missed due to lack of time [3].
24

25 In this paper, we propose a CAD system for the intervertebral disc dis-
26 eases for the lumbar region of the spine where the low back pain most
27 commonly occurs [4]. The lumbar region of the human spine, contain-
28 ing 5 vertebrae $v = \{L1, L2, L3, L4, L5\}$ and the intervertebral discs $d =$
29 $\{T12 - L1, L1 - L2, L2 - L3, L3 - L4, L4 - L5, L5 - S1\}$, is the portion
30 of the spine where pain is generally felt and pathologies occur [4]. A T2-
31 weighted MR image of the lumbar spine is shown in Figure 1-(a).
32

33 According to the nomenclature and classification of lumbar disc pathol-
34 ogy document [5], the discs are classified as: normal, congenital/development
35 variant, degenerative lesion, infection, neoplasia, and morphologic variant.
36 The discs may be categorized into one or more diagnostic classes because
37 multiple pathologies may occur at the same time. In this study, we concen-
38 trate on the following classes:
39

40 **Normal:** The intervertebral discs are classified as normal if there is no mor-
41 phological, degenerative, developmental, or adaptive changes.
42

43 **Degenerative/traumatic lesion:** The annular tear, herniation including
44 protrusion/extrusion, degeneration are considered as degenerative/traumatic
45 lesion.
46

47 *Annular tear:* It is the separation between annular fibers and avul-
48 sion of fibers from their vertebral body insertions.
49

50 *Herniation:* The disc material, including nucleus, cartilage, frag-
51 mented apophyseal bone, and annular tissue, migrates through the an-
52

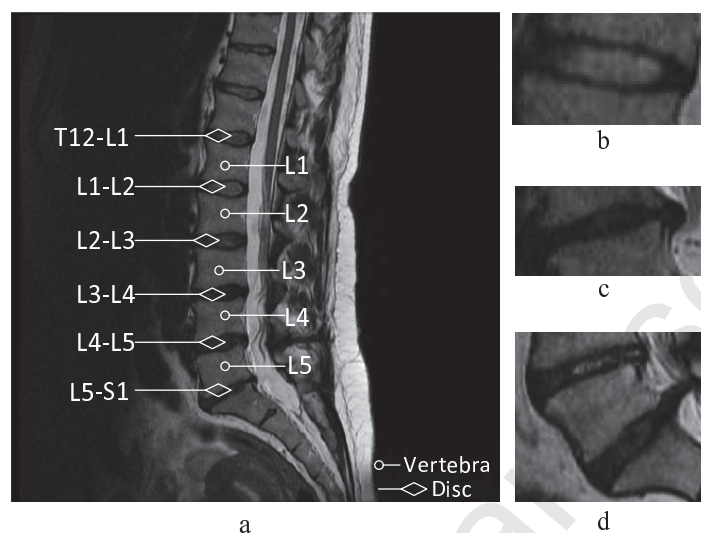


Figure 1: a) A T2-weighted lumbar MR image where the discs and vertebrae are marked. b) A normal disc, c-d) Discs diagnosed as degenerative disc diseases including desiccation, herniation, and annular tear.

annular tear and it is called herniation. Herniation is also classified into subcategories like protrusion and extrusion.

Degeneration: Desiccation (drying out of the water in pulposus), fibrosis, narrowing of the disc space, diffuse bulging of the annulus beyond the disc space, and extensive fissuring are types of degeneration. Degeneration may happen because of aging, trauma, and annular tears.

Magnetic Resonance (MR) imaging is generally used for the diagnosis of disc pathologies in clinical practice. The normal discs are ellipse-shaped and bright in the T2-weighted MR images, while the degenerated and herniated discs are dark and have arbitrary shapes (Figure 1(b)-(d)).

We propose a CAD system that automatically diagnoses the degenerative disc disease in the lumbar intervertebral discs at the mid-sagittal 2D MR images. In order to make the diagnosis, our system considers many aspects of the discs including the intensity values, shapes, texture, and context. These aspects are combined under a machine learning framework.

The system has 3 basic steps: First, the intervertebral discs are automatically detected and labeled with our previous method [6, 7]. Then, the

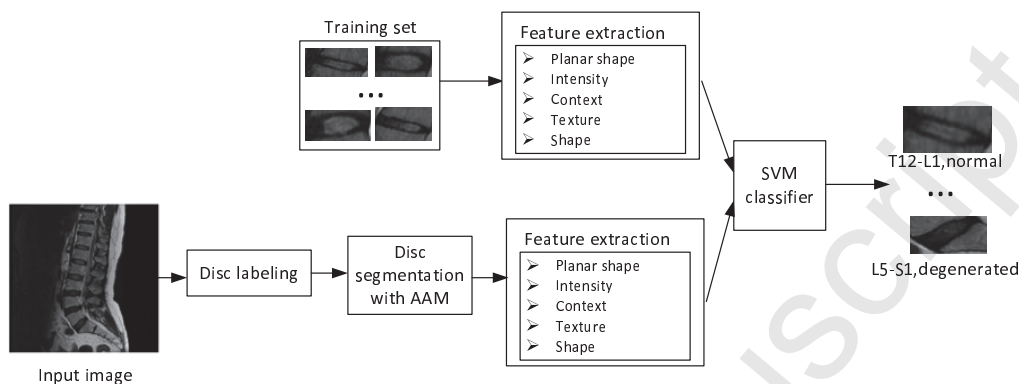


Figure 2: The flowchart of the proposed system.

discs are segmented with Active Appearance Models (AAM) [8]. Third, different types of image features are extracted with various methods and they are trained/tested with Support Vector Machines (SVM). Figure 2 shows the basic steps of our system, which is evaluated on a dataset that includes clinical MR images of 102 subjects.

Our system has several contributions: First, the difference image, which is calculated by using both T1-weighted and T2-weighted MR images, is introduced for incorporating intensity information. The difference images give crucial information about the pathologies and eliminate the problems caused by imaging artifacts. In addition, we propose an automatic initialization system for the AAM using the windows detected for disc localization. The system considers different types of features like intensity, texture, whole shape, and context together for evaluating the disc pathology. To the best of our knowledge, this is the first study that uses difference images and uses an automatic initialization system.

The rest of paper is organized as follows: In Section 2, related work is presented. The disc labeling and segmentation processes are described in Section 3.1 and 3.2, respectively. Section 3.3 includes the extraction of shape, texture, intensity, and context information. The learning and training phase of the system is presented in Section 3.4. Section 4 includes the experiments and the validation of the method. Finally, we provide the concluding remarks in Section 5.

2. Related Work

In the literature, there are many studies for detection [9, 10], labeling [11, 12], and segmentation [13, 14] of the vertebrae and the intervertebral discs. However, the number of studies for the CAD of degenerative disc diseases is limited. In addition, these methods were tested on small datasets.

Chwialkowski et al. [15] presented an intensity based method for detecting the intervertebral discs and analyze the correlation between the intensity distribution and disc abnormality. Tsai et al. [16] employed B spline curves to approximate the normal disc boundary and the extracted convex and concave features determined the herniation ratio on transverse sections. Michopoulou et al. [17] presented a texture based characterization system for cervical intervertebral disc degeneration from sagittal MR images with a Least Squares Minimum Distance classifier.

Alomari et al. [18] proposed a probabilistic model for detecting abnormal discs from T2-weighted images using Gibbs distribution. They modeled the abnormal disc appearance, location, and the context information about distance with Gaussian models. In [19], a similar system for the diagnosis of desiccation which uses only the appearance and distance information was developed. In these studies the shape of the discs were ignored. [20] proposed a method for the diagnosis of herniation that segments the discs with a gradient vector flow active contour model and used a Bayesian-based classifier with a Gibbs distribution. However, the whole disc shape was not fully utilized; only the minor and major axis of the segmented disc shape were used as shape information.

Ghosh et al. [21] presented a majority voting system for the lumbar herniation diagnosis that uses intensity, planar shape features, and texture features extracted by Gray level co-occurrence matrix. The system was tested on a dataset containing 35 subjects and the accuracy of the system was 94.86%. [3] proposed a new system that employs raw intensity features and texture information (extracted with Gabor filters and LBP) besides the intensity and planar shape features in [21]. The system was tested on a dataset containing 35 subjects and the accuracy was 98.29%. Hao et al. [22] proposed an active learning based degeneration diagnosis system that takes the segmented disc images as input and uses texture and intensity information for SVM classification. The system was tested on 27 subjects and achieved over 90% accuracy on average.

The methods described above mainly concentrated on the intervertebral

1
2
3
4
5
6
7
8
9
10
11
12
13
14
15
16
17
18
19
20
21
22
23
24
25
26
27
28
29
30
31
32
33
34
35
36
37
38
39
40
41
42
43
44
45
46
47
48
49
50
51
52
53
54
55
56
57
58
59
60
61
62
63
64
65

disc intensity information. They also use different types of information like texture, planar shape (width and height of the disc), and distance in order to evaluate the disc abnormalities. They are tested on smaller data sets and containing at most 65 subjects [20]. Our method differs from those studies in that it uses information more effectively about the intervertebral discs and it is tested on a larger data set containing 102 subjects.

3. Method

3.1. Automatic Disc Localization and Labeling

The labeling of the discs is crucial before the automated diagnosis because in clinical practice the abnormalities are reported with the disc label. The lumbar intervertebral discs are labeled by the method of [6, 7].

The method finds the center location and the label of each lumbar disc d_i where $1 \leq i \leq 6$. Since a sliding window technique is used, each detected disc d_i is tightly surrounded by a window W_{d_i} . The window W_{d_i} is used for the automatic initialization of the AAM for segmenting the disc d_i .

The method works as follows:

1. The spinal cord is detected by subtracting T1-weighted MR images from T2-weighted images and using morphological operations.
2. Pyramidal Histogram of Oriented Gradients (PHOG) and Image Projection Descriptors are extracted from the MR images with the sliding window technique.
3. The extracted features are trained and tested with Sequential Minimal Optimization (SMO). During testing each candidate window is given a score which shows the probability of including a lumbar disc.
4. The final disc labels are determined by using a graphical model that uses the score values of SMO and context information like orientation and distance of discs.

3.2. Disc Segmentation

One of the major problems of the popular segmentation algorithms (e.g., snakes, level sets, AAM) is the initialization. Since they are iterative algorithms that use local image information, the initialization affects the segmentation results. We propose a novel automatic initialization method for segmenting the discs by utilizing the window information extracted in the disc labeling step.

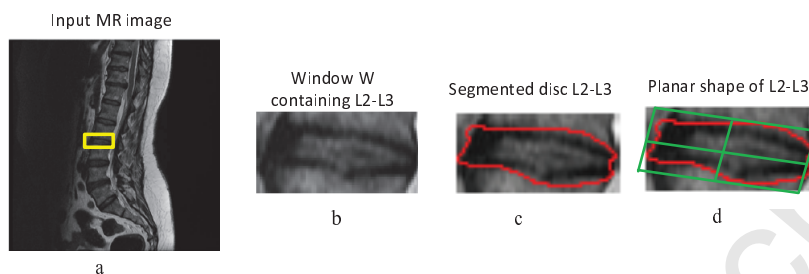


Figure 3: a-A target input MR image and the yellow rectangle shows the window W detected, b-the window W including the disc d_i . c-Disc d_i segmented with AAM. d- A bounding box including the segmented disc d_i and its major x and y axes.

The outputs of the automatic disc labeling step are the locations (center points) and labels of the lumbar intervertebral discs d_i and the windows $W_d = W_{d_1}, \dots, W_{d_6}$ containing those discs. The windows W_d provide crucial information for the segmentation step because they approximately give the disc boundary and the initial contour is placed into the window. The output of the AAM is the segmented disc image S_{d_i} where $d_i \in d$ and $1 \leq i \leq 6$. Note that each intervertebral disc d_i is trained for segmentation separately because their shapes are not similar.

Figure 3-a shows an example of lumbar MR image where the detected window W_{d_3} is delineated with a yellow rectangle. The window W_{d_3} shown in Figure 3-b is used for initialization of the AAM. The output of the segmentation algorithm is shown in Figure 3-c.

We use AAM for segmentation because the intensity and gradient based algorithms like active contours and snakes may not work properly in the cases where the disc is dark or has abnormal boundary like desiccation and herniation. Since the AAM have a shape-based training phase, the abnormal cases are also learned with the healthy ones and they are successfully segmented.

3.3. Feature Extraction

In clinical practice, the intensity values, shape, context, and height of the intervertebral discs are evaluated all together for the diagnosis of diseases. Different from the studies in the literature, we take all of this information into account and extract various features from the intervertebral disc images for the automated diagnosis system.

3.3.1. Planar Shape

The planar shape of the discs, indicated by the height and width of the discs in 2D midsagittal images, is one of the indicators of disc degeneration [23] because when the disc collapses due to aging and drying out, the height of the disc decreases [24].

We extract the average width and height of the each disc d_i using the segmentation result S_{d_i} . We use the average width, height and their ratio as the planar shape features. Note that the abnormality detection studies in the literature [3],[21] use the length of the main axes of the discs instead of average height and width values. However, the major x and y axes lengths may not be so much affected in some cases like herniation where only the part near to the spinal cord has a small length. Therefore, using the average lengths instead of major axis lengths is a better indicator of the abnormality. Figure 3-d shows the bounding rectangle and the major x and y axes of the segmented disc d_3 .

3.3.2. Intensity

The inner part of the normal intervertebral discs has a high water content. However, there may be drying or water loss because of desiccation and herniation. In T2-weighted MR images, the healthy discs with high water content are very bright and the abnormal discs with low water content are very dark. Therefore, the T2-weighted MR images are used for diagnosis in clinical practice. The studies in the literature generally use the raw disc intensity information. However, there may be imaging artifacts or the intensity values may change because of the calibration of the MR devices. Therefore, instead of using only the raw intensity values in T2-weighted images, we propose using the difference image D_{d_i} calculated by

$$D_{d_i} = T2(S_{d_i}) - T1(S_{d_i}); \quad (1)$$

where $T1$ and $T2$ are the normalized T1-weighted and T2-weighted MR disc images. The intensity histogram of the difference image D_{d_i} and the mean of the intensity values at pixels in D_{d_i} are used as the intensity features.

3.3.3. Context

The context information is important in clinical practice because the comparison of neighboring discs in terms of intensity provides important information about the pathologies. Therefore, we use the intensity information at

the neighboring lumbar intervertebral discs. First, the average, maximum, and minimum of the average of the intensity values in T2-weighted segmented disc images except the target disc are determined. Then, they are subtracted from the mean intensity of the target image as follows

$$\begin{aligned} c_1 &= \text{mean}(T2(S_{d_i})) - \max(T2(S_{d_k})), \\ c_2 &= \text{mean}(T2(S_{d_i})) - \min(T2(S_{d_k})), \\ c_3 &= \text{mean}(T2(S_{d_i})) - \text{mean}(T2(S_{d_k})), \end{aligned} \quad (2)$$

where $1 \leq k \leq 6$ and $i \neq k$. *max*, *min* and *mean* are the functions that give the maximum, minimum and the average of the mean intensity values of the neighboring five lumbar discs d_k , respectively. The value c_1 is high if the target disc d_i is darker than the neighboring lumbar discs d_k and c_2 is high if d_i is brighter than d_k .

3.3.4. Texture

Texture of the discs contains important information about the disc pathologies. We use Local Binary Patterns (LBP) [25] for extracting the texture features of the discs. The calculation of LBP for the pixel c with pixel neighborhood containing P sampling points is

$$LBP(x) = \sum_{i=0}^{P-1} s(g_i - g_c) * 2^i, \quad (3)$$

$$s(n) = \begin{cases} 1 & \text{if } n > 0, \\ 0 & \text{otherwise,} \end{cases} \quad (4)$$

where g_i is the intensity value of the pixel at i . The occurrences of the LBP features in the disc images S_{d_i} are collected into a histogram and this histogram is used as the texture descriptor.

3.3.5. Shape Information

The shape of the discs demonstrates the some abnormalities like herniation. In order to extract the shape information, we use moments for representing the global characteristics and geometric features of shape. Hu's moment invariants [26] are employed as the shape descriptor which are invariant to rotation, scaling and translation. Hu's moment invariants $H1, H2, \dots, H7$ are calculated as

$$H_1 = \eta_{2,0} + \eta_{0,2}, \quad (5)$$

$$H_2 = (\eta_{2,0} - \eta_{0,2})^2 + 4\eta_{1,1}^2, \quad (6)$$

$$H_3 = (\eta_{3,0} - 3\eta_{1,2})^2 + (3\eta_{2,1} - \eta_{0,3})^2 \quad (7)$$

$$H_4 = (\eta_{3,0} + \eta_{1,2})^2 + (\eta_{2,1} + \eta_{0,3})^2 \quad (8)$$

$$H_5 = (\eta_{3,0} - 3\eta_{1,2})(\eta_{3,0} + \eta_{1,2}) [(\eta_{3,0} + \eta_{1,2})^2 - 3(\eta_{2,1} + \eta_{0,3})^2] + \\ (3\eta_{2,1} - \eta_{0,3})(\eta_{2,1} + \eta_{0,3})[3\eta_{3,0} + \eta_{1,2})^2 - (\eta_{2,1} + \eta_{0,3})^2] \quad (9)$$

$$H_6 = (\eta_{2,0} - \eta_{0,2}) [(\eta_{3,0} + \eta_{1,2})^2 - (\eta_{2,1} + \eta_{0,3})^2 + 4\eta_{1,1}(\eta_{3,0} + \eta_{1,2})(\eta_{2,1} + \eta_{0,3})] \quad (10)$$

$$H_7 = (3\eta_{2,1} - \eta_{0,3})(\eta_{3,0} + \eta_{1,2}) [(\eta_{3,0} + \eta_{1,2})^2 - (3\eta_{2,1} + \eta_{0,3})^2] + \\ (\eta_{3,0} - 3\eta_{1,2})(\eta_{2,1} + \eta_{0,3}) [(3\eta_{3,0} + \eta_{1,2})^2 - (\eta_{2,1} + \eta_{0,3})^2], \quad (11)$$

where $\eta_{p,q}$ is a normalized central moment of order $p + q$. The 7 moment values H are used as shape descriptors. The moment values incorporate knowledge about the global shape and geometric features of the discs.

3.4. Training

The extracted planar shape, intensity, context, texture, and shape features are combined with concatenation to obtain the final descriptor. For training the SVM, we use Sequential Minimal Optimization (SMO) [27] algorithm that contains many optimizations designed to speed up the training algorithm and convergence under degenerate conditions.

4. Experiments

The system is tested and validated on a clinical MR dataset containing MR volumes for the spinal lumbar column of 102 subjects. The MR images are gathered from 3 different devices which are all 1.5T. In the dataset, there are T1-weighted sagittal, T2-weighted sagittal and T2-weighted axial acquisition protocols for each subject. The midsagittal (median sagittal slice) registered T2-weighted and T1-weighted MR images are used for the experiments.

There are lumbar MR images of 102 subjects in the dataset and there are totally $102 \times 6 = 612$ lumbar intervertebral discs. 349 of the discs are normal and 263 of them are diagnosed with degenerative disc disease. The discs are labeled and diagnosed by a radiologist for the ground truth.

Table 1: The performance metrics of [21], [3], and our method.

	Accuracy	Sensitivity	Specificity
The method of [21]	70.75	75.6	64.3
The method of [3]	86.28	87.4	84.8
Our method	92.81	94.6	89.8

The dataset containing 612 discs is randomly divided into 6 subsets each containing 102 discs and we performed 6 sub-experiments. In each sub-experiment, the discs in 5 subsets ($102 \times 5 = 510$ discs) are used for training and the discs in the other subset are tested. So, the training and testing instances are always distinct and each disc is tested once by the system.

We use accuracy (ACC), specificity (SPE) and sensitivity (SEN) metrics for performance evaluation which are defined as:

$$\text{Accuracy} = (TP + TN) / (TP + TP + FN + FP), \quad (12)$$

$$\text{Specificity} = TN / (TN + FP), \quad (13)$$

$$\text{Sensitivity} = TP / (TP + FN), \quad (14)$$

where TP is the number of true positives, TN is the number of true negatives, FN is the number of false negatives and FP is the number of false positives.

In order to compare our system with the state of the art, we implement the methods of [3] and [21] which report their accuracy rate as 98.29% and 94.86% for the dataset containing 35 subjects, respectively. We implement the systems according to the techniques and parameters given in the papers. The training and test instances and the number of sub-experiments are same with our method for a fair comparison. Note that, although the methods of [3] and [21] are proposed for herniation diagnosis, they are expected to diagnose the degenerative disc disease because they use intensity and shape features that give information about degeneration and annular tear and herniation is a also type of degenerative disc disease.

The performance of our method, and the methods of [3] and [21] are shown in Table 1. The accuracy of our method is 92.81%. The accuracy of the method presented in [21], which uses intensity, texture and planar shape features, is 70.75%. The accuracy of the method presented in [3] that uses more texture descriptors and raw intensity features besides the features in

Table 2: The performance metrics of each individual feature type for the method of [3], [21] and our method.

Features used in Our Method				Features used in [3]			
	ACC(%)	SEN	SPE		ACC(%)	SEN	SPE
Intensity (Difference images)	89.54	0.96	0.82	Raw Features	86.44	0.88	0.84
Shape (avg axis)	59.64	0.93	0.14	LBP	70.01	0.80	0.57
Shape(Hu's)	71.57	0.72	0.71	Gabor	59.64	0.80	0.33
Texture (LBP)	70.10	0.80	0.57	Planar Shape	55.02	1.00	0
Context	73.20	0.83	0.61	Intensity	57.02	1.00	0
				GLCM	71.08	0.78	0.62

[21] is 86.28%.

We perform a feature comparison through Receiver Operating Characteristic (ROC) curves in Figure 4 and the accuracy rates are given in Table 2. Figure 4-(a) shows the ROC curves of our system and the ROC curves of the individual features used in our system. In our system, the intensity features that use difference images perform well and it is followed by context, shape and texture features. Figure 4-(b) shows the ROC curves of the features used in [3]. It is observed that the raw intensity features have the highest accuracy in [3] and the overall accuracy of [3] is similar to the accuracy of raw features as reported in [3]. The shape and texture information encoded by GLCM and LBP features have similar accuracy. The shape and intensity features have 0 specificity and all of the instances are classified as having no disease. It indicates that they do not provide sufficient information alone. Also, our planar shape feature, which uses the average width and height after segmentation, has higher accuracy than the planar shape feature of [21],[3] which uses only the ratio of major axis lengths.

The accuracy rate of [3] is higher than [21] as expected because it is an extended version that uses more information. The results show that in [3] the texture features extracted with Gabor filters and LBP and raw intensity features increase the accuracy of the system. The accuracy of our system is higher than [3] and [21]. This indicates that the information incorporated with context features, shape descriptors and difference images provides an important accuracy gain to our system.

Finally, we performed another experiment in order to evaluate performance of the difference images. In this experiment, we use all of the features

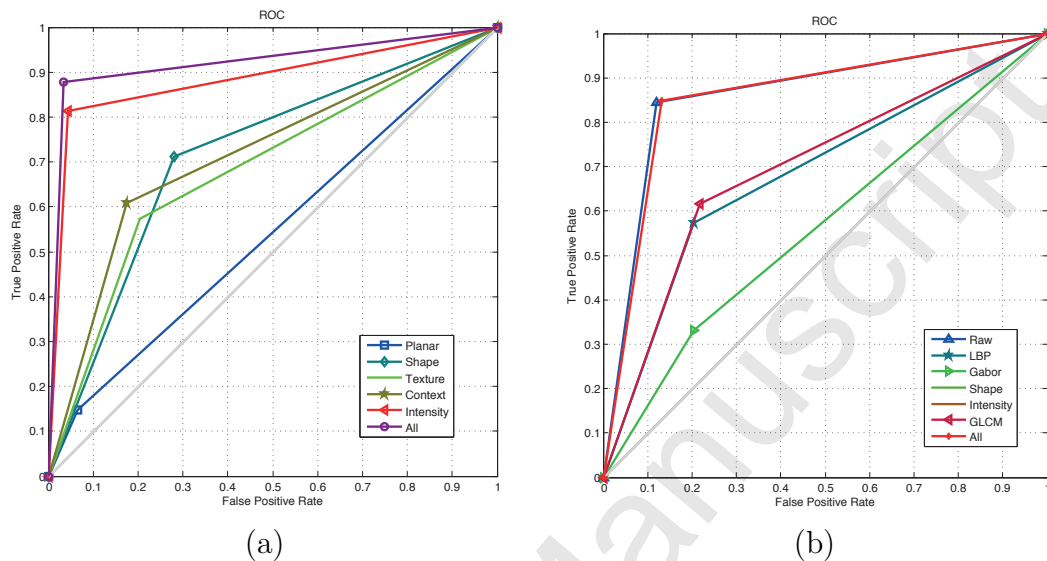


Figure 4: (a) ROC for our method and individual features, (b) ROC for the method of [3] and individual features.

(planar shape, context, texture, and shape) except intensity for degeneration diagnosis. The accuracy rate without difference image based features is 84.31% which is lower than the accuracy 92.81% when all features are used. This experiment show the affectiveness of the difference images in a CAD system for degenerative disc disease.

Note that the accuracy rates reported in [21] and [3] are slightly different than the accuracy rates when they are run on our dataset. This may be caused by several reasons. First, the raw intensity features mostly affect the accuracy of [21] and [3] and our dataset may have low image quality compared to their dataset. Also, the dataset of [21] and [3] consists of 35 images and the data variability of cases may be low in their dataset.

5. Conclusions

We present a novel method for the automated diagnosis of degenerative disc diseases using a machine learning framework. The method first localizes and segments the intervertebral lumbar discs. Then shape, context, intensity, and texture information about the discs is extracted with various techniques and they are learned with SVM.

1
2
3
4
5
6
7
8
9 We present an effective automated initialization technique by using the
10 detected windows during localization. In this way, AAM produces successful
11 segmentation results even in arbitrary shaped discs. The incorporation of in-
12 tensity information with difference images eliminates the problem of imaging
13 artifacts. Image moments provide knowledge about the geometrical features
14 about the disc shape. In addition, context features are employed for making
15 comparison with the neighboring lumbar intervertebral discs.
16
17

18 The dataset that we use to validate our system includes the clinical lum-
19 bar MR images of 102 subjects. It is the largest dataset used for evaluation.
20 We compare our system with the methods of [21, 3] which have the highest
21 accuracy in the literature. The experimental results show that our system
22 has 92.8% accuracy which is comparable with the state of the art.
23
24

25 References

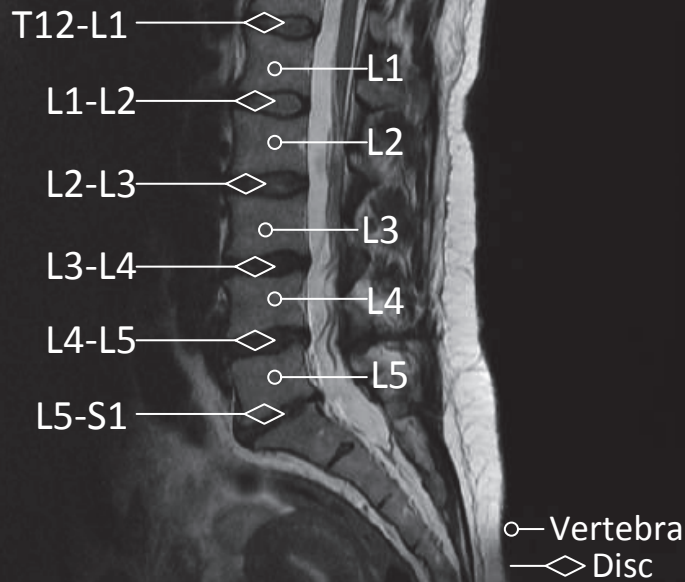
- 26
27 [1] X. Luo, R. Pietrobon, S. X. Sun, G. G. Liu, L. Hey, Estimates and
28 patterns of direct health care expenditures among individuals with back
29 pain in the United States., *Spine* 29 (2004) 79–86.
30
31 [2] A. Patel, A. Ogle, Diagnosis and management of acute low back pain,
32 *Am Fam Physician* 61 (2000) 1789–1790.
33
34 [3] S. Ghosh, R. S. Alomari, V. Chaudhary, G. Dhillon, Composite features
35 for automatic diagnosis of intervertebral disc herniation from lumbar
36 mri, in: *Conf Proc IEEE Eng Med Biol Soc.*, 2011, pp. 5068–5071.
37
38 [4] National Institute of Neurological Disorders and Stroke, Low back pain
39 fact sheet, <http://www.ninds.nih.gov/disorders/backpain/>, 2011.
40
41 [5] D. F. Fardon, P. C. Milette, Nomenclature and Classification of Lumbar
42 Disc Pathology, *Spine* 26 (2001) 93–113.
43
44 [6] A. B. Oktay, Y. S. Akgul, Simultaneous localization of lumbar vertebrae
45 and intervertebral discs with svm-based mrf, *Biomedical Engineering,*
46 *IEEE Transactions on* 60 (2013) 2375–2383.
47
48 [7] A. B. Oktay, Y. S. Akgul, Localization of the lumbar discs using machine
49 learning and exact probabilistic inference, in: *Proc. of the 14th Int. Conf.*
50 *Medical Image Comput. and Computer-Assisted Intervention*, volume
51 6893 of *Lecture Notes in Computer Science*, Springer, 2011, pp. 158–
52 165.
53
54
55
56
57
58

- 1
2
3
4
5
6
7
8
9 [8] T. F. Cootes, C. J. Taylor, D. H. Cooper, J. Graham, Active shape
10 models-their training and application, *Comput. Vis. Image Underst.* 61
11 (1995) 38–59.
12
13 [9] B. M. Kelm, S. K. Zhou, M. Suehling, Y. Zheng, M. Wels, D. Comaniciu,
14 Detection of 3d spinal geometry using iterated marginal space learning,
15 in: *Proc. of the Int. MICCAI Cof. on Medical Comp. Vis.: recognition*
16 *techniques and applications in medical imaging*, 2011, pp. 96–105.
17
18 [10] Y. Zhan, D. Maneesh, M. Harder, X. S. Zhou, Robust mr spine detection
19 using hierarchical learning and local articulated model, in: *Proc. of the*
20 *15th Int. Conf. on Medical Image Computing and Computer-Assisted*
21 *Intervention*, MICCAI’12, 2012, pp. 141–148.
22
23 [11] B. Glocker, J. Feulner, A. Criminisi, D. R. Haynor, E. Konukoglu, Au-
24 tomatic localization and identification of vertebrae in arbitrary field-
25 of-view ct scans, in: *Proc. of the 15th Int. Conf. on Medical Image*
26 *Computing and Computer-Assisted Intervention*, 2012, pp. 590–598.
27
28 [12] R. S. Alomari, J. J. Corso, V. Chaudhary, Labeling of lumbar discs
29 using both pixel- and object-level features with a two-level probabilistic
30 model, *IEEE Trans. on Medical Imaging* 30 (2011) 1–10.
31
32 [13] S.-H. Huang, Y.-H. Chu, S.-H. Lai, C. L. Novak, Learning-based verte-
33 bra detection and iterative normalized-cut segmentation for spinal MRI,
34 *IEEE Transactions on Medical Imaging* 28 (2009) 1595–1605.
35
36 [14] S. K. Michopoulou, L. Costaridou, E. Panagiotopoulos, R. D. Speller,
37 G. Panayiotakis, A. Todd-Pokropek, Atlas-based segmentation of de-
38 generated lumbar intervertebral discs from mr images of the spine, *IEEE*
39 *Trans. Biomed. Engineering* 56 (2009) 2225–2231.
40
41 [15] M. Chwialkowski, P. Shile, R. Peshock, D. Pfeifer, R. Parkey, Auto-
42 mated detection and evaluation of lumbar discs in mr images 2 (1989)
43 571–572.
44
45 [16] M.-D. Tsai, S.-B. Jou, M.-S. Hsieh, A new method for lumbar herni-
46 ated inter-vertebral disc diagnosis based on image analysis of transverse
47 sections, *Computerized Medical Imaging and Graphics* 26 (2002) 369 –
48 380.
49
50
51
52
53
54
55
56
57
58
59
60
61
62
63
64
65

- 1
2
3
4
5
6
7
8
9 [17] S. Michopoulou, I. Boniatis, L. Costaridou, D. Cavouras, E. Panagiotopoulos, G. Panayiotakis, Computer assisted characterization of cervical intervertebral disc degeneration in mri, *Journal of Instrumentation* 4 (2009) P05022.
- 10
11
12
13
14
15 [18] R. S. Alomari, J. J. Corso, V. Chaudhary, G. Dhillon, Abnormality detection in lumbar discs from clinical mr images with a probabilistic model, in: *Proceedings of 23rd International Congress and Exhibition on Computer Assisted Radiology and Surgery (CARS 2009)*, 2009.
- 16
17
18
19
20
21 [19] R. S. Alomari, J. J. Corso, V. Chaudhary, G. Dhillon, Desiccation diagnosis in lumbar discs from clinical mri with a probabilistic model, in: *Proc. of the 6th IEEE Int. Conf. on Symposium on Biomedical Imaging: From Nano to Macro, ISBI'09, 2009*, pp. 546–549.
- 22
23
24
25
26
27 [20] R. S. Alomari, J. J. Corso, V. Chaudhary, G. Dhillon, Toward a clinical lumbar cad: herniation diagnosis, *International Journal of Computer Assisted Radiology and Surgery* 6 (2011) 119–126.
- 28
29
30
31
32 [21] S. Ghosh, R. S. Alomari, V. Chaudhary, G. Dhillon, Computer-aided diagnosis for lumbar mri using heterogeneous classifiers, in: *IEEE International Symposium on Biomedical Imaging*, 2011, pp. 1179–1182.
- 33
34
35
36 [22] S. Hao, J. Jiang, Y. Guo, H. Li, Active learning based intervertebral disk classification combining shape and texture similarities, *Neurocomputing* 101 (2013) 252–257.
- 37
38
39
40
41 [23] A. Neubert, J. Fripp, C. Engstrom, D. Walker, R. Schwarz, S. Crozier, Automatic quantification of 3d morphology and appearance of intervertebral discs in high resolution mri, 2013.
- 42
43
44
45 [24] F. Kolstad, G. M. nd Kjell Arne Kvistad, ystein P. Nygaard, G. Leivseth, Degeneration and height of cervical discs classified from mri compared with precise height measurements from radiographs 55 (2005) 415–420.
- 46
47
48
49
50 [25] T. Ojala, M. Pietikinen, D. Harwood, Performance evaluation of texture measures with classification based on kullback discrimination of distributions, in: *Proc. of the 12th IAPR Int. Conf. on Pattern Recognition*, 1994, pp. 582 – 585.
- 51
52
53
54
55
56
57
58
59
60
61
62
63
64
65

1
2
3
4
5
6
7
8
9
10
11
12
13
14
15
16
17
18
19
20
21
22
23
24
25
26
27
28
29
30
31
32
33
34
35
36
37
38
39
40
41
42
43
44
45
46
47
48
49
50
51
52
53
54
55
56
57
58
59
60
61
62
63
64
65

- [26] M. K. Hu, Visual Pattern Recognition by Moment Invariants, IRE Transactions on Information Theory IT-8 (1962) 179–187.
- [27] J. C. Platt, Advances in kernel methods, MIT Press, Cambridge, MA, USA, 1999, pp. 185–208.



a



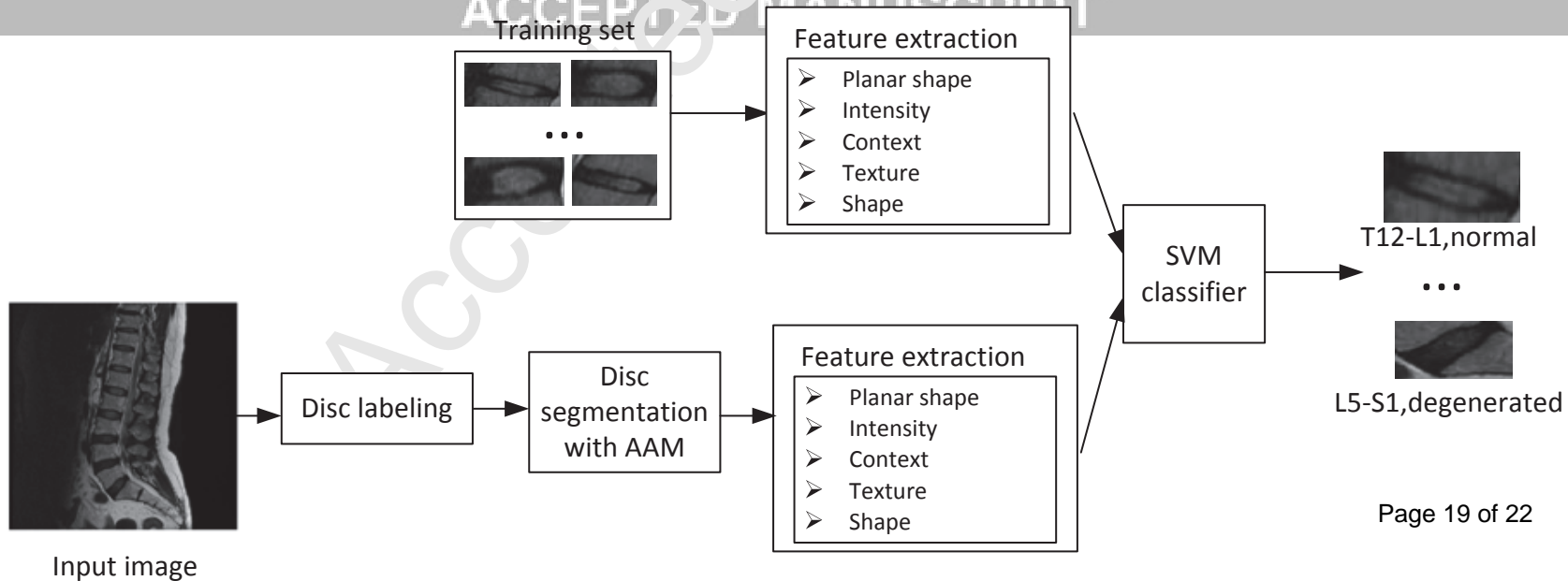
b



c



d



Input MR image

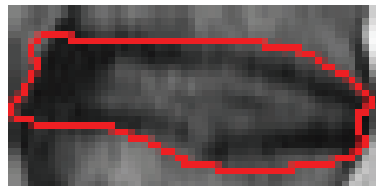


a

Window W
containing L2-L3

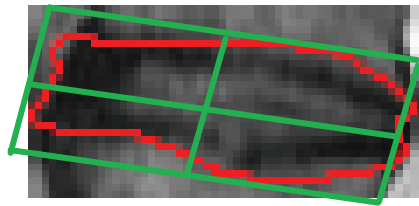
b

Segmented disc L2-L3



c

Planar shape of L2-L3



d

